Anal. Bioanal. Electrochem., *Vol.* 9, *No. 2, 2017, 245-265*

Analytical &
Bioanalytical
Electrochemistry

Full Paper

Curcumine Longa: Green and Sustainable Corrosion Inhibitor for Aluminum in HCl Medium

N. K. Gupta, M. A. Quraishi,* P. Singh, V. Srivastava, K. Srivastava, C. Verma and A. K. Mukherjee

Department of Chemistry, Indian Institute of Technology, Banaras Hindu University, Varanasi 221005, India

*Corresponding Author, Tel.: +91-9307025126; Fax: +91- 542- 2368428

E-Mail: maquraishi@rediffmail.com; maquraishi.apc@itbhu.ac.in

Received: 2 December 2016 / Received in revised form: 10 February 2017 / Accepted: 9 March 2017 / Published online: 31 March 2017

Abstract- The inhibition effect of Curcumine Longa (CUR) on the corrosion of aluminum in presence of 1 M HCl solution was studied by weight loss, Potentiodynamic polarization, electrochemical impedance spectroscopy (EIS), quantum chemical calculations and SEM techniques. Weight loss and electrochemical results showed that inhibition efficiency of CUR increases with increase in the concentration and attained a maximum value of 89.60% at 100 ppm concentration. Polarization study revealed that CUR acts as mixed type inhibitor whereas EIS study showed that the CUR inhibits aluminum corrosion by getting adsorbed at metal/ electrolyte interfaces which followed the Langmuir adsorption isotherm. SEM study confirmed the film forming ability of CUR on the aluminum surface. Quantum chemical calculations study was performed to provide insight into adsorption behavior of CUR on the aluminum surface. Experimental and theoretical results were in good agreement and well complimented to each other.

Keywords- Aluminum, Corrosion Inhibitor, Weight loss, Electrochemical measurements, Quantum calculations

1. INTRODUCTION

Aluminum is the second most abundant metal after iron on the earth. Due to its strength, low density and high electrical and thermal conductivity, it is used in construction, packing,

and transportation field and making electronic gadgets [1,2]. It is well known that aluminum is protected by the formation of compact adherent passive oxide film on its surface. But this film is amphoteric in nature, so consequently metal dissolves in the acidic and basic medium having a pH less than 5 and greater than 9 [3]. Hydrochloric solution is one of the most effective acids for the pickling and electrochemical etching of aluminum and its alloys [4]. However, chloride ions of this acid break the passive oxide film and initiate the pitting corrosion [5,6]. Among several methods available for combating corrosion of aluminum, the most cost effective and practical one is the use of chemical inhibitors [7,8]. It is well known that effective corrosion inhibitors are the organic compounds that contain oxygen, sulfur, and/or nitrogen as polar groups and conjugated double bonds in their structure [9-11]. The inhibition efficiency of these compounds generally depends on the chemical structure of the compound, charged surface of the metal and the type of interaction between the metal surface and inhibitor molecule [12-14].

In the literature, several organic compounds such as amines [15,16], carbonyl compounds [17], thiosemicarbazide derivatives [18], hydrazine derivatives [19], amino acids [20], drugs [21], Schiff bases [22,23], ionic liquids [24], surfactants [25-28], pyridine derivatives [29], benzotriazole derivatives [30], chalcogen derivatives [31], oximes [32] have been reported as effective corrosion inhibitor for the aluminum and its alloys in acidic media. But most of the available synthesized inhibitors are very expensive and hazardous to living beings and environment, and they should be replaced with new environmentally friendly inhibitors. So, recently natural products and their extracts have become an important alternative to toxic inhibitors because they are environmentally acceptable, readily available and renewable source for a wide range of corrosive environments [33-34]. As a contribution to the current interest on environmentally friendly, green, corrosion inhibitors, the present study investigates the inhibition effect of CUR on aluminum corrosion in 1 M HCl medium. Chemically CUR is 1,7-bis(4-Hydroxy-3-methoxyphenl)-1,6-heptadiene-3,5-dione. It is the principal curcuminoid of the popular Indian spice turmeric, which is a member of the ginger family (Zingiberaceae). Curcumin is a polyphenolic compound which can exist in at least two tautomeric forms, i.e. keto and enol forms and among them enol form is most stable in solid as well as solution phase [35]. CUR has a long history of use in Ayurvedic medicine due to its antioxidant, anti-inflammatory, antiviral and antifungal actions [36]. The choice of CUR as a corrosion inhibitor for aluminum was inspired from the facts that it is non-toxic, natural product that contains heteroatom, polar functional group, and conjugated double bonds which will support the adsorption of CUR on aluminum surface. Kairi et al have used CUR for corrosion inhibition of mild steel in 1 M HCl solution and have achieved efficiency of 79.81% at 80 ppm [37]. Susui et al used curcumine extract for protection of aluminum in simulated concrete pore solution which comprise of natural sea water environment (3.5%

NaCl) [38] but so far no literature is present on the use of CUR as corrosion inhibitor for aluminum in hydrochloric acid.

2. EXPERIMENTAL

2.1. Materials

All the weight loss, electrochemical and surface analysis experiments were performed on aluminum 1060 specimens having the following chemical composition (wt.%): 0.25% Si, 0.35% Fe, 0.05% Cu, 0.03% Mn, 0.03% Mg, 0.05% Zn, 0.03% Ti, 0.05% V and balance Al. The compound CUR was purchased from Sigma Aldrich and used as it is. The structure of the CUR molecule is given in Fig. 1. The aggressive solutions of 1 M HCl was prepared by dilution of analytical grade 37% HCl with double distilled water.

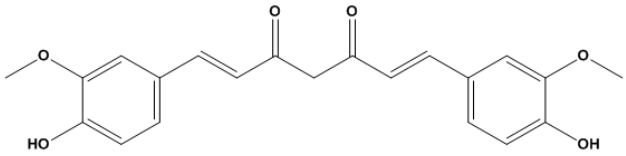

Fig. 1. Chemical Structure of curcumine longa molecule

2.2. Methods

2.2.1. Weight Loss Measurements

Weight loss experiments were performed on the aluminum coupons having composition described above with dimension 2.5 cm×2.0 cm×0.25 cm according to the standard methods [39]. Before the weight loss experiments the aluminum coupons were cleaned by silicon carbide abrasive paper (500–1200 grade), washed with distilled water, cleaned with acetone, dried and kept in moisture free desiccator. Then coupons were weighed accurately and immersed in 100 ml of 1 M HCl solution in the absence and presence of different concentrations of CUR for 3 hours. After that the aluminum coupons were taken out rinsed with double distilled water, cleaned in acetone, dried at ambient temperature and finally weighed accurately. All experiments were carried out in triplicate and average of weight loss was reported to ensure more accurate result. Corrosion rate (mg $cm^{-2}h^{-1}$) for aluminum was calculated by using following equation [39].

$$C_R = \frac{W}{At} \quad (1)$$

Where W is the average weight loss of an aluminum coupon, A is the total area of aluminum coupon and t is immersion time i.e. 3 h. After calculating corrosion rate, the

percent inhibition efficiency (η%) and surface coverage (θ) were calculated from following equations [40]

$$\eta\% = \frac{C_R - C_{R(i)}}{C_R} \times 100 \quad (2)$$

$$\theta = \frac{C_R - C_{R(i)}}{C_R} \quad (3)$$

Where CR and $C_{R(i)}$ are the values of the corrosion rates (mg $cm^{-2}h^{-1}$) of aluminum in absence and presence of CUR, respectively.

2.2.2. Electrochemical measurements

Electrochemical experiments were performed on the aluminum strip as a working electrode of size 6 cm×1cm with total exposed area of 1 cm^2 in a conventional three-electrode Pyrex glass cell with a platinum counter electrode (exposed area 1 cm^2) and a saturated calomel electrode (SCE) as reference. Electrochemical measurements were performed in absence and presence of different concentration of CUR by using a Gamry Potentiostat/Galvanostat (ModelG-300) connected with a personal computer with EIS software Gamry Instruments Inc., USA. The electrochemical experiment results were analyzed by electrochemical software Echem Analyst 5.0 software package. Before starting the experiments, the working electrode was immersed in 1 M HCl solution for 15 min to set up the balanced state E_{ocp} in aerated solution at 308 K. Then working electrode was allowed to corrode freely to measure its corrosion potential as a function of time for 200 s. When steady-state OCP corresponding to the corrosion potential (E_{corr}) of the working electrode was obtained then the EIS and polarization experiments were performed [41].

EIS experiments were carried out using AC signals of amplitude 10 mV peak to peak at the open circuit potential in the frequency range 100 kHz–0.01 Hz and then data obtained were fitted to appropriate circuits using the computer program Echem Analyst 5.0. Potentiodynamic polarization curves were performed by automatically changing the electrode potential from (-250 to +250) mV SCE versus OCP at a scan rate of 1 mVs^{-1} and then linear Tafel segments of anodic and cathodic curves were extrapolated to obtain corrosion current densities (Icorr) [42].

2.2.3. Surface morphology using scanning electron microscopy (SEM)

The aluminum strips of size 2.5×2×0.025 cm were immersed in 1 M HCl in absence and presence of optimum concentration (100 ppm) of CUR for 3 h. Thereafter, the specimens

were taken out, washed with double distilled water, dried at ambient temperature and mechanically cut into 1 cm^2 size for SEM analysis. SEM study was carried out at an accelerating voltage of 5 kV and 5 KX magnification on a Ziess Evo 50 XVP instrument.

2.2.4. Quantum chemical calculations

Quantum chemical calculations were performed with complete geometry optimization by using standard Gaussian 03 W software package. All calculations were done by DFT/B3LYP theory by using 6-31 g (d,p) orbital basis sets.

3. RASULTS AND DISCUSSION

3.1. Weight loss method

3.1.1. Effect of inhibitor concentration

Effect of concentration of CUR was studied by performing weight loss experiment on aluminum specimen in 1 M HCl with and without different concentrations of CUR for 3 h immersion time at 308 K. Variation of the inhibition efficiency with concentration is shown in Fig. 2 and various weight loss parameters such as corrosion rate (C_R), surface coverage (θ) and corresponding inhibition efficiency (η%) were calculated from the weight loss experiment are listed in Table 1.

Table 1. The weight loss measurement parameters for aluminum in 1 M HCl containing different concentrations of inhibitor

Inhibitors	**Concentrations (ppm)**	**Corrosion rate (mg cm^{-2} h^{-1})**	**Surface coverage (θ)**	**η%**
Blank	0.0	3.76	-	-
	25	1.50	0.60	60.17
	50	0.83	0.77	77.87
	75	0.53	0.85	85.84
	100	0.40	0.89	89.38

In Fig. 2 it can be seen that on increasing concentration of CUR inhibition efficiency increases and reaches to a maximum value of 82.4% at 100 ppm concentration. After that no appreciable increase in inhibition efficiency was observed above this concentration which indicates that the protective effect of CUR is due to the adsorption of its molecule on metal

surface which impede the dissolution of latter by blocking its corrosion sites and hence decreasing the corrosion rate [43].

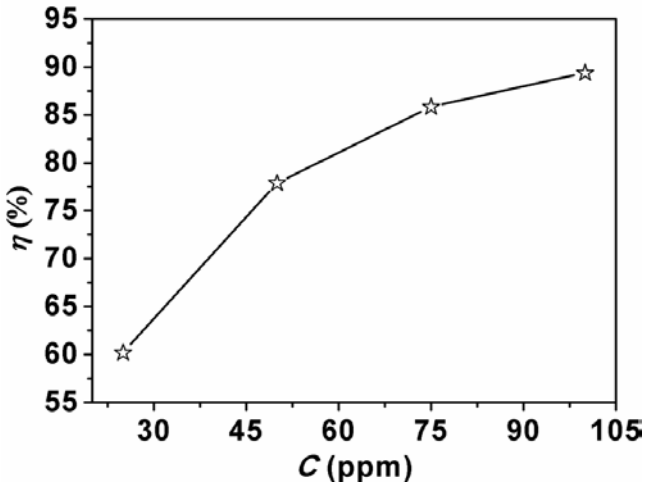

Fig. 2. Variation of inhibition efficiency with inhibitor concentration at 308 K

3.1.2. Effect of temperature

The weight loss experiments were performed at different temperatures from 308 to 338 K in order to study the effect of temperature on inhibition efficiency and to calculate activation energy of corrosion process. Temperature investigation is also important to have an idea about the stability of the inhibitor film. Fig. 3 shows the variation of inhibition efficiency of CUR at optimum concentration (100 ppm) of CUR with temperature. Inspection of Fig. 3 reveals that inhibition efficiency decreases with increase in temperature. The increase in corrosion rate on increasing temperature can be attributed due to etching, rupture and desorption of inhibitor molecules [44].

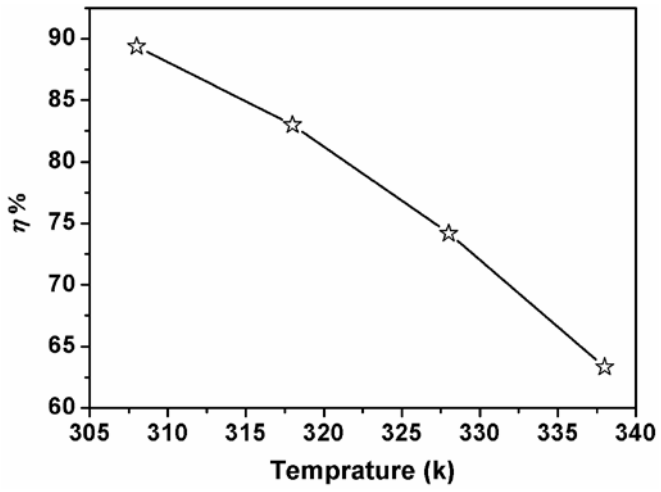

Fig. 3. Variation of inhibition efficiency with temperature at optimum concentration of CUR

The dependency of corrosion rate on temperature can be best represented by the Arrhenius equation given by [45]:

$$\log(C_R) = \frac{-E_a}{2.303RT} + \log \lambda \qquad (٤)$$

Where Ea is the apparent activation energy, R is the molar gas constant, T is the absolute temperature (K) and λ is the Arrhenius pre-exponential factor, known as frequency factor. Arrhenius plot (Fig. 4) of log(CR) *vs* 1000/T for corrosion of aluminum in 1 M HCl solution gave straight line with regression coefficient (R2) value close to one.

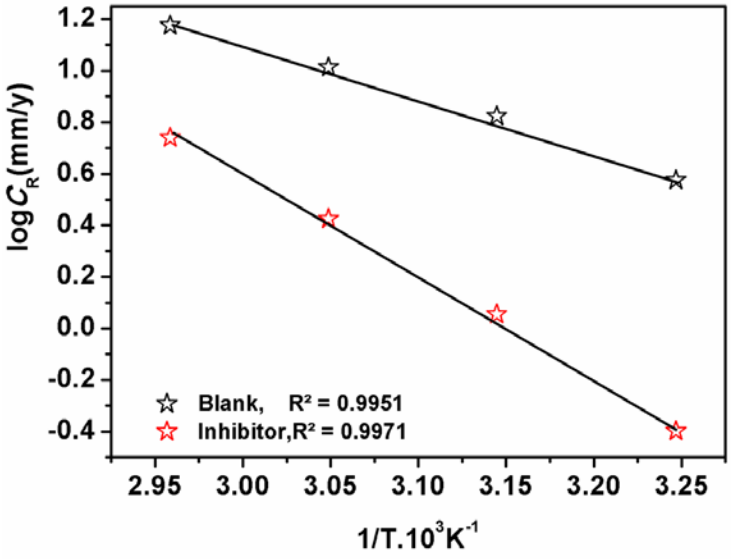

Fig. 4 Arrhenius plots of log CR versus 1000/T for aluminum corrosion in 1 M HCl

The values of Ea for corrosion of aluminum in absence and in presence of optimum concentration of CUR were calculated from the slope of the lines and are shown in Table 2. It is clear from the Table 2 that the value of Ea is higher in presence of inhibitor than that in its absence. This increase of Ea in presence of inhibitor indicates that adsorbed inhibitor film on aluminum surface increases the energy barrier for corrosion reaction [46].

Table 2. Activation energy for aluminum dissolution in 1 M HCl in the absence and presence of an optimum concentration of inhibitor

Inhibitor	***E*a (kJmol^{-1})**
Blank	39.76
inhibitor	75.60

3.1.3 Adsorption isotherm

The adsorption isotherm can be used to get important information about the interaction of inhibitor molecules and metal surface. Adsorption behavior of inhibitor can be explained by using two type of interaction: physisorption and chemisorptions. These interactions depend on the chemical structure of the inhibitor molecule, the temperature of medium, electrochemical potential, the charge, and nature of the metal [47]. The adsorption of organic inhibitor molecules from the aqueous solution can be considered as a quasi-substitution process between the organic inhibitor in the aqueous phase [Inh(sol)] and water molecules adsorbed on the metal surface [H_2O(ads)]. This situation can be represented by the following equilibrium [48]: $\mathrm{Inh(sol)} + \mathrm{X\ H_2O(ads)} \rightleftharpoons \mathrm{Inh(ads)} + \mathrm{X\ H_2O(sol)}$

Where X is the number of water molecules replaced by one inhibitor molecule. In this situation adsorption of inhibitor is taking place with desorption of water molecule from metal surface.

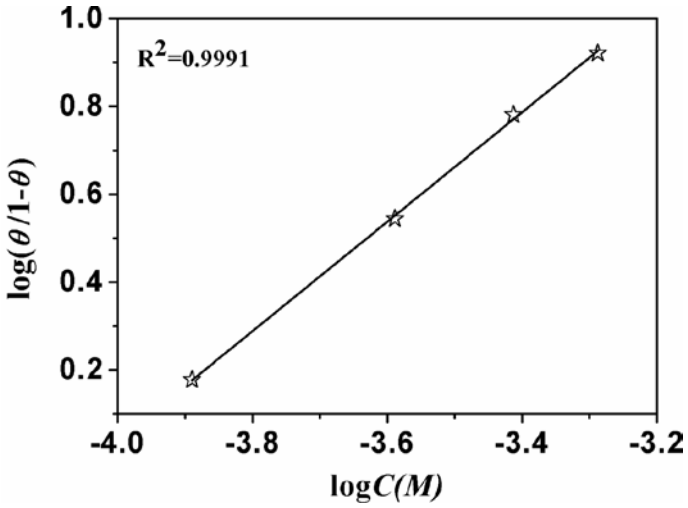

Fig. 5. Langmuir adsorption isotherms of Aluminum in 1 M HCl in presence of inhibitor

In the present study, degree of surface coverage at 308K with different concentration of inhibitors were fitted to different adsorption isotherms including Flory–Huggins, Langmuir, Freundlich and Temkin isotherms but the best fit was obtained by Langmuir adsorption isotherms which give a straight line between log (θ/1−θ) *vs* log $C_{(inh)}$ (Fig. 5) with regression coefficient 0.9991 which is very close to unity, conforming the validity of this approach [49]. Langmuir adsorption isotherm is given by:

$$K_{ads}C = \frac{\theta}{1-\theta} \tag{5}$$

Where θ is the surface coverage, C is the inhibitor concentration, K_{ads} is the equilibrium constant of adsorption process. Values of K_{ads} at different concentration of inhibitors were calculated from weight loss experiment data and are given in Table 3.

Table 3. The values of K_{ads} and ΔG^0_{ads} of inhibitors for mild steel in 1 M HCl at 308 K

***C*(ppm)**	**K_{ads}(10^3 M^{-1})**	**ΔG_{ads} (kJ mol^{-1})**
25	11.6	-34.27
50	11.7	-34.66
75	12.0	-34.02
100	16.1	-35.11

It is well established that K_{ads} represents the strength of interaction between adsorbent and adsorbate and it is clear from the Table 3 that the value of K_{ads} is high which may be due to strong interaction between inhibitor molecule and aluminum surface [50]. Value of K_{ads} is increasing with increase in concentration which means that there is more adsorption on increasing concentration. The adsorption free energy (ΔG^0_{ads}) of the CUR on aluminum surface can be calculated using following equation [50]:

$$\Delta G^{o}_{ads} = -RT \ln(55.5K_{ads}) \quad (6)$$

Where the value 55.5 represents the concentration of water in solution expressed in mol/L. The calculated values of ΔG_{ads}^0 are given in Table 3. The large and negative value of ΔG^0_{ads} suggests that the adsorption of CUR molecule on the aluminum surface in 1 M HCl solution is a spontaneous process. It is well established that the value of ΔG^0_{ads} around or less than 20 KJ mol^{-1} represents physisorption and around or greater than 40 KJ mol^{-1} is considered as chemisorption [51,52]. In our study, the value of the ΔG^0_{ads} ranges from -35.11 KJ mol^{-1} to -34.02 kJ mol^{-1} suggesting that it is a case of physiochemical mode of adsorption [40].

3.2. Electrochemical measurements

3.2.1. Potentiodynamic polarization

The various electrochemical phenomenon including electrochemical polarization and passivation can be explained by using Potentiodynamic polarization method. Polarization measurements are suitable for analyzing the progress and mechanisms of the anodic and cathodic half reactions as well as studying the effect of inhibitor on anodic and cathodic half reactions separately [53,54]. The anodic and cathodic polarization curves for the corrosion of aluminum in 1 M HCl solution in the absence and presence of varying concentrations of CUR

at 35 °C are shown in Fig. 6 and electrochemical parameters such as corrosion potential (E_{corr}), corrosion current density (i_{corr}), cathodic Tafel slope (β_c), and inhibition efficiency η(%) determined from polarization curves are given in Table 4. It is well reported in the literature that if shift in E_{corr} value is greater than 85 mV, a chemical compound can be designated as an anodic or a cathodic type inhibitor otherwise it will be considered as mixed type inhibitor. In present case, the shift in E_{corr} value is not significant i.e. less than 85 mV, suggesting that the CUR is a mixed type inhibitor [41].

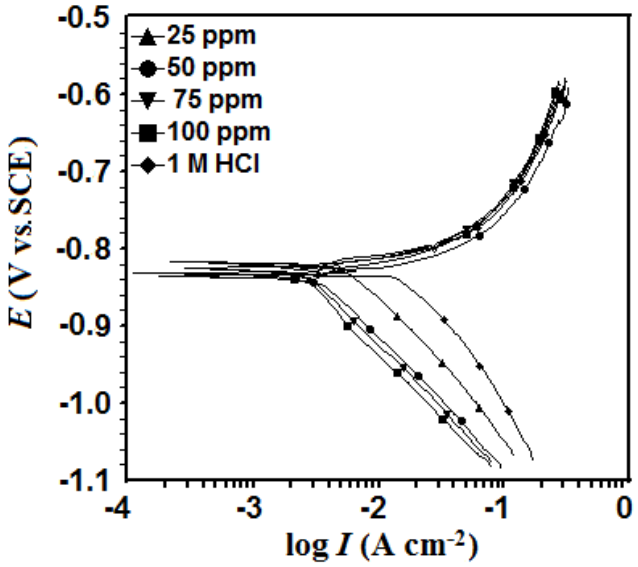

Fig. 6. Potentiodynamic polarization curves for aluminum in 1 M HCl in the absence and presence of different concentrations of inhibitor

As can be seen from the Fig. 6 that the cathodic polarization curves give rise to Tafel lines and owing to the fact that cathodic polarization curves are parallel it can be inferred that the hydrogen evolution reaction is activation controlled and presence of inhibitor does not affect the mechanism of hydrogen evolution. It is also important to note that in anodic domain it is difficult to recognize the linear Tafel regions so the corrosion current density values in the presence and the absence of inhibitor in HCl solutions were determined by the extrapolation of cathodic Tafel slopes to the respective corrosion potentials. Similar fitting method has been widely used for aluminum in HCl [27] and H_3PO_4 [55] solutions in the presence of organic inhibitors. According to data of Table 4, corrosion current density of aluminum decreases and inhibition efficiency increases with the increasing inhibitor concentration. This result may be related to the adsorption of the CUR molecules at the active sites of aluminum surface which impeded the corrosion rate. The increase in inhibition efficiency with increase in concentration of inhibitor molecule indicates more inhibitor

molecule adsorption on metal surface thus providing wider surface area coverage and act as adsorption inhibitor.

Table 4. Potentiodynamic polarization parameters for aluminum dissolution in 1 M HCl with and without inhibitor

***C*(ppm)**	**E_{corr} (mV versus SCE)**	**i_{corr} (µA $cm^{-2)}$**	**βc (mV /dec)**	**η%**
Blank	-883	17090	202	-
25	-883	5567	171	67.4
50	-835	3139	157	81.6
75	-824	2243	155	86.8
100	-829	1940	153	88.6

3.2.2. Electrochemical impedance spectroscopy (EIS)

The inhibition efficiency of CUR on aluminum was examined by electrochemical impedance spectroscopy. The impedance spectra of aluminum in 1 M HCl solution in the absence and presence of four different concentrations of inhibitor were recorded at 35 ˚C and shown in Fig. 7. The impedance spectra consist of a large capacitive loop at high frequency (HF) followed by a large inductive loop at low frequency (LF) values.

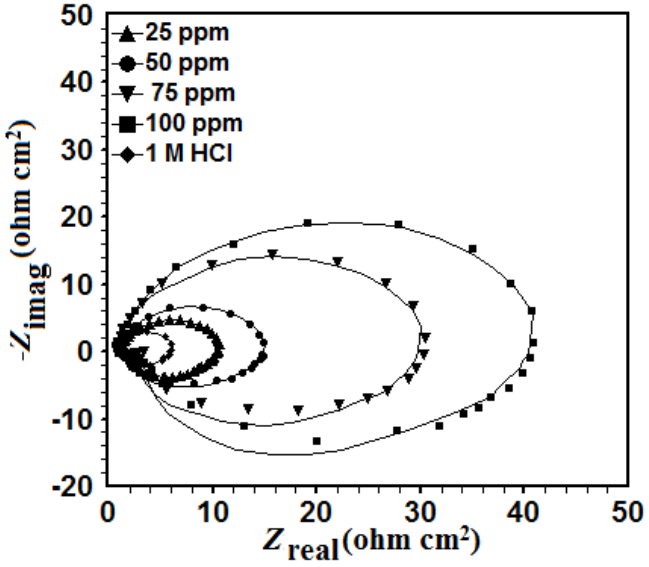

Fig. 7. Nyquist diagrams for aluminum in 1 M HCl in the absence and presence of different concentrations of inhibitor

In general cases small inductive loop at LF is always observed for aluminum in HCl [56-58]. Usually the diameter of inductive loop is smaller to more extent than that of capacitive loop at HF. However, in the present system, the size of inductive loop is almost equal to that of capacitive loop due to which the whole diagram appears an elliptic shape. Similar impedance plots have been reported of aluminum [59] and aluminum alloys [60,61] in HCl media with organic inhibitors. On comparing impedance spectra of inhibited solution at different concentrations with that of uninhibited 1 M HCl solution (blank) it is clear that the shape of spectra is maintained throughout all tested concentrations, indicating that there is almost no change in the corrosion mechanism due to the inhibitor addition [62].

According to Bessone et al. [63] and Brett [64], the capacitive loop at high frequency could be due to the oxide layer on aluminum metal surface. In the experiments, it is reasonable to assume that the electrode surface has been covered with an oxide layer because of the ex situ pretreatment of the electrode. In fact, it is very difficult to produce an oxide free Al surface and even if such surface is produced, it is repassivated very fast by O_2 [65]. The capacitive loop at HF corresponds to the interfacial reactions, particularly, the reaction of aluminum oxidation at the metal/oxide/electrolyte interface [41] which indicates that the corrosion of aluminum is mainly controlled by a charge transfer process, and usually related to the charge transfer of the corrosion process and double layer behavior.

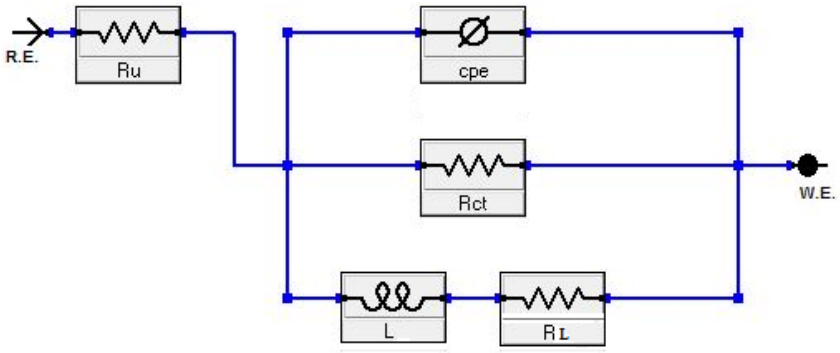

Fig. 8. Equivalent circuit used to fit the EIS

On the other hand, the cause of the large inductive loop at low frequency is still not clear. Adsorbed charged intermediates and ions like $[H^+]_{ads}$, Cl^-, O^{2-} or inhibitor species may result in an inductive loop [62]. This is more pronounced when the intermediates are strongly adsorbed on the electrode surface. It may also be due to the re-dissolution of the oxide layer surface [66] or Al-dissolution [60] at low frequencies.

Nevertheless, the sizes of both capacitive and inductive loops increase significantly with an increase in inhibitor concentration which suggests that the impedance of inhibited substrate increases with inhibitor concentration. Noticeably, these HF loops are not perfect

semicircles which can be attributed to the frequency dispersion as a result of the roughness and inhomogeneous of electrode surface [67]. The EIS results are calculated by the equivalent circuit shown in Fig. 8. R_u, R_{ct}, R_L and R_p are the solution resistance, charge transfer resistance, inductive resistance and polarization resistance, respectively. *CPE* is constant phase element. *L* is the inductance, which is intimately associated with the inductive loop. The inhibition efficiency (η%) was calculated by applying the following equation:

$$\eta\% = \frac{R_p^i - R_p^0}{R_p^i} \times 100 \quad (7)$$

Table 5. Electrochemical parameters calculated form EIS measurements for aluminum in 1 M HCl in the absence and presence of an optimum concentration of inhibitor at 308 K

***C*(ppm)**	R_s (Ω cm^2)	R_{ct} (Ω cm^2)	R_L (Ω cm^2)	***L*** (Ω cm^2)	R_P (Ωcm^2)	***CPE*** (μF cm^{-2})	**η%**
Blank	0.736	5.510	0.220	1.205	0.211	64	-
25	1.068	9.486	1.019	1.924	0.919	45	77.0
50	0.827	13.93	1.237	1.645	1.136	32	81.4
75	0.694	30.29	2.143	2.974	2.001	29	89.4
100	0.861	39.78	2.155	6.461	2.044	14	89.6

All the impedance parameters are listed in Table 5. Inspection of Table 5 reveals that both Rct and Rp values increases prominently with the concentration of CUR which indicates that the electrode exhibits slower corrosion in the presence of inhibitor. The decrease in CPE value in case of inhibitor with that in blank solution (without inhibitor), which can be due to decrease in local dielectric constant and/or an increase in the thickness of the electrical double layer, suggests that the inhibitor molecules function by adsorption at the metal/solution interface [68,69]. It is clear from Table 5 that inhibition efficiency increases with the concentration of inhibitor and reaches upto 89.6% which again confirm that CUR exhibit good inhibitive performance for aluminum in 1 M HCl solution. Inhibition efficiencies obtained from weight loss, potentiodynamic polarization and EIS are in good agreement.

3.3. Scanning electron microscopy (SEM)

Characterization of the metal surface was carried out by SEM technique in order to support our findings. The SEM image of aluminum samples were taken after 3 h immersion

in 1 M HCl solution in the absence and presence of 100 ppm of inhibitor and those images are shown in Fig. 9(a) and 9(b) respectively. The micrograph of specimen dipped in blank solution shown in Fig. 9(a) clearly reveals that the metal surface was strongly damaged in the absence of inhibitor due to the metal dissolution in aggressive solution. Furthermore, the corrosion products appear very uneven and cube-shaped morphology, and the surface layer is rather rough. On other hand the micrograph of inhibited specimen shown in Fig. 9(b) reveals that there is much less damage on the aluminum surface, which further confirms the inhibition ability of CUR.

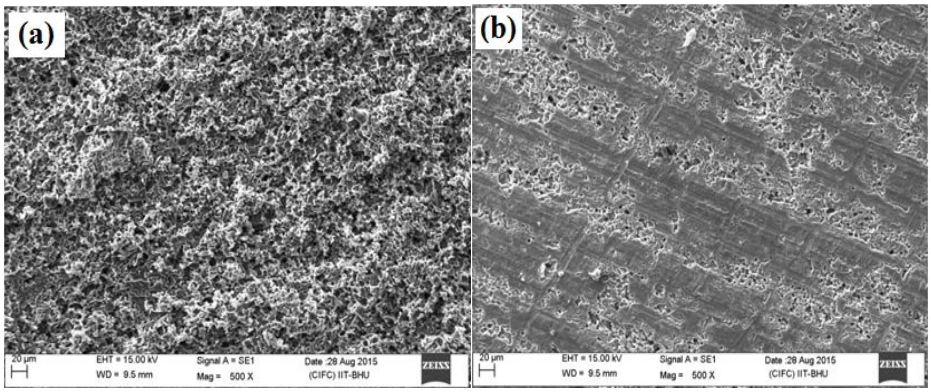

Fig. 9. SEM micrographs of aluminum surface: (a) after 3 h of immersion in 1 M HCl solution; (b) after 3 h of immersion at optimum concentration of curcumine longa

3.4. Quantum chemical calculations

To support experimental finding of the present work that CUR exhibited high inhibition efficiency in the 1 M HCl, the quantum chemical calculations were performed on neutral as well as protonated forms of the CUR. Figs. 10 and 11 represent the optimized, highest occupied frontier molecular orbital (E_{HOMO}) and lowest occupied frontier molecular orbital (E_{LUMO}) diagrams of the neutral and protonated CUR and corresponding computed parameters are given in Table 6. Because, organic inhibitor molecules having heteroatoms get easily protonated in acid solution and therefore quantum chemical calculations of the protonated form of the CUR along with neutral form have been considered in the present study.

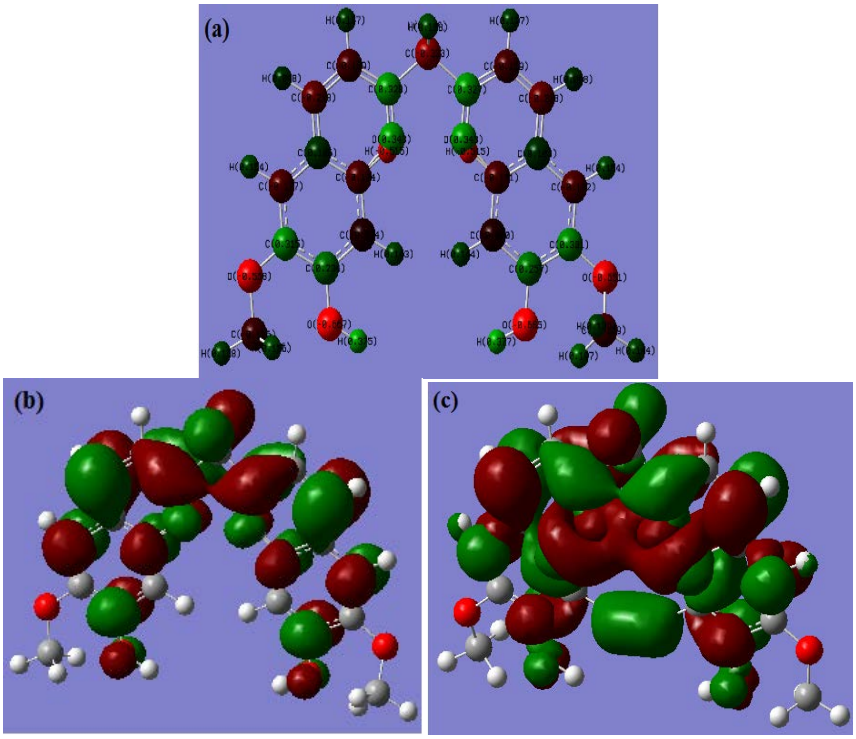

Fig. 10. Geometric optimized (a), highest occupied molecular orbital [E_{HOMO},(b)] and lowest unoccupied molecular orbital [E_{LUMO}, (c)] of neutral CUR

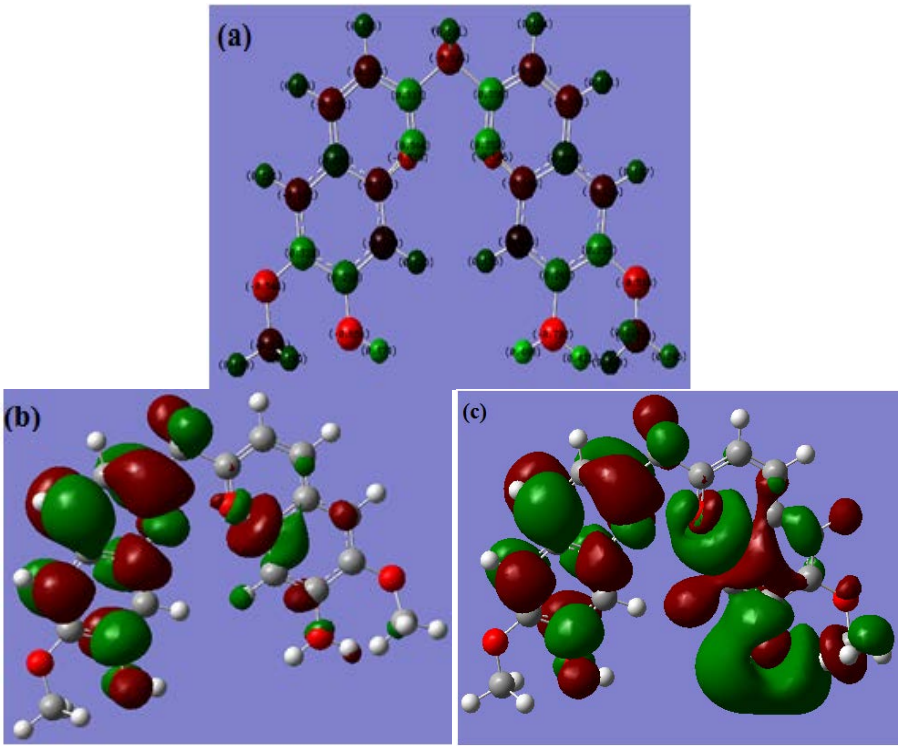

Fig. 11. Geometric optimized (a), highest occupied molecular orbital [E_{HOMO},(b)] and lowest unoccupied molecular orbital [E_{LUMO} (c)] of protonated CUR

From frontier molecular electron distribution diagrams (Fig. 10 and 11) it can be seen that electrons are almost uniformly distributed on compete CUR molecule which indicates that almost complete part of the molecules involves in electrons transfer and acceptation i.e. adsorption [70,71]. Generally, high value of E_{HOMO} is related with electron donating ability of the inhibitor molecule during adsorption process. In the present study, the values of E_{HOMO} for neutral and protonated CUR were found comparatively high which suggests that CUR has strong electron donating tendency while inhibitor being adsorb onto the metallic surface [70-72]. While, the value of E_{LUMO} is related with electron accepting tendency of the inhibitor molecule. Comparatively a lower value of E_{LUMO} for CUR in the present study suggests that it has strong tendency to accept electrons into its antibonding molecular orbitals from the metallic surface during adsorption process [70-72].

The energy band gap (ΔE, E_{LUMO}-E_{HOMO}) is another important parameter related with the chemical reactivity and thereby inhibition efficiency of the inhibitor molecule. In general, a low value of ΔE related with high chemical reactivity and therefore high inhibition efficiency. In the present study, value of ΔE is very low (Table 6) for both neutral and protonated forms of CUR suggesting that CUR has potential tendency of adsorption over the metallic surface [73,74]. From the results depicted in Table 6 it can be seen that values of dipole moment of CUR in protonated and neutral forms are much higher as compare to the dipole moment of water (1.85 Debye). This finding suggests that CUR has stronger tendency of adsorption on the mild steel surface in aqueous acid solution as compare to the water and therefore CUR replace the water from the metallic surface and form inhibitor film which isolates the metal from aggressive acid solution and inhibits its corrosion. Two other quantum chemical calculation parameters namely global hardness (ρ) and global softness (σ) those are associated with values of E_{HOMO}, E_{LUMO} and ΔE were derived for neutral as well as protonated forms of CUR. Obviously, a high value of hardness associated with low chemical reactivity and therefore low inhibition efficiency, while a high value of softness generally related with the high chemical reactivity [75-78]. In our present study, the low values of hardness and high values of softness for protonated as well as neutral forms of inhibitor indicate that the CUR has high chemical reactivity and therefore exhibited high inhibition efficiency as was found from experimental means.

Table 6. Quantum chemical parameters calculated for neutral and protonated forms of CUR

Curcumine Longa	**HOMO (Hartree)**	**LUMO (Hartree)**	**Δ*E* (Hartree)**	**μ (Debye)**	**Hardness (ρ)**	**Softness (σ)**
Neutral	-0.10626	-0.05704	0.04922	4.6318	0.02461	40.633
Protonated	-0.20316	-0.18207	0.02109	15.3644	0.010545	94.831

3.5. Inhibition Mechanism

Adsorption is known to be the key mechanism of inhibition action, and it might be suggested that the inhibitor molecules are adhered to the metal surface, which decreases the surface area at which cathodic and anodic reactions take place. The adsorption process is mainly influenced by the number of adsorption active centers and their charge density in the inhibitor molecules and the nature of metal/solution interface [79]. It is believed that adsorption is the first step in the mechanism of corrosion inhibition process in aggressive acid medium. Inhibitor molecules can adsorb on metal surface by: (i) attraction of cationic form with negatively charged metal surface (ii) via chemisorption mechanism involving the sharing of lone pair electrons between the oxygen atom and metal atom (iii) through π-electron interactions between the aromatic ring of the molecule and the metal surface. The mechanism for anodic dissolution of aluminum in HCl solution can be represented by following steps [22]:

$Al + Cl^- \rightarrow AlCl^-_{ads}$ (a)

$AlCl^-_{ads} + Cl^- \rightarrow AlCl_2^+ + 3e^-$ (b)

Whereas the cathodic hydrogen evolution follows the steps:

$H^+ + e^- \rightarrow H_{ads}$ (c)

$H_{ads} + H_{ads} \rightarrow H_2$ (d)

As discussed above the value of standard adsorption free energy (ΔG^0_{ads}) indicates that the adsorption is mainly the physiochemisorption. Consequently, the adsorption mechanism is presented. In aqueous acidic solutions, CUR molecule exists either as neutral molecule or in the protonated form. These protonated CUR molecules can electrostatically interact with $AlCl^-_{ads}$ species which are formed in step (a). This phenomenon is attributable to stabilization of adsorbed halides ions by means of electrostatic interactions with the inhibitor molecules, resulting in greater surface coverage [80]. The protonated molecules are also adsorbed on the cathodic sites of aluminum in competition with the hydrogen ions (step(c)) which prevent the hydrogen ions from participating in the cathodic reaction of the corrosion and hence impede the hydrogen gas evolution taking place in step (d) [50].

4. CONCLUSION

Curcumin effectively inhibits the corrosion of aluminum in 1 M HCl solutions. The inhibition efficiency of CUR increases with its concentration and attains a maximum value of 89.38. The adsorption of CUR on aluminium surface obeys Langmuir adsorption isotherm. Polarization curves illustrate that the studied compound acted as mixed type inhibitor. EIS spectra showed a large capacitive loop at high frequencies followed by a large inductive loop at low frequency values. EIS plot also indicated that the addition of inhibitors

increases the charge-transfer resistance for the corrosion process. The inhibition efficiencies obtained from weight loss and electrochemical (EIS and Tafel polarization) methods are in reasonable agreement. SEM analysis also supported the formation of film on the metal surface. Quantum chemical calculations provided more detailed account on mode of donor- accepter interactions between metal and inhibitor molecule. The Quantum chemical calculation also revealed that degree of inhibition efficiency of CUR is related to the donation and retro donation of electrons from inhibitor to metal and metal to inhibitor molecule.

Acknowledgements

Gupta *et al.* is thankful to Department of Chemistry, Indian institute of Technology Banaras Hindu University for providing instrumentation facilities.

REFERENCES

[1] R. Rosliza, W. B. W. Nik, and H. B. Senin, Mater. Chem. Phys. 107 (2008) 281.
[2] A. S. Fouda, A. A. Al-Sarawy, F. S. Ahmed, and H. M. El-Abbasy, Corros. Sci. 51 (2009) 485.
[3] S. Safak, B. Duran, A. Yurt, and G. T. ˘lu, Corros. Sci. 54 (2012) 251.
[4] R. Xiao, K. Yan, J. Yan, and J. Wang, Corros. Sci. 50 (2008) 1576.
[5] H. Oh, J. Lee, H. Ahn, Y. Jeong, N. Park, S. Kim, and C. S. Chi, Mater. Sci. Eng. A 449–451 (2007) 348.
[6] B. Zaid, D. Saidi, A. Benzaid, and S. Hadji, Corros. Sci. 50 (2008) 1841.
[7] C. M. A. Brett, I. A. R. Gomes, and J. P. S. Martins, Corros. Sci. 36 (1994) 915.
[8] S. Zein, and E. Abedin, J. Appl. Electrochem. 31 (2001) 711.
[9] A. S. Fouda, A. A. Al-Sarawy, F. S. Ahmed, and H. M. El-Abbasy, Corros. Sci. 51 (2009) 485.
[10] A. Yurt, and Ö. Aykın, Corros. Sci. 53 (2011) 3725.
[11] S. M. A. E. Haleem, S. A. E. Wanees, E. E. A. E. Aal, and A. Farouk, Corros. Sci. 68 (2013) 1.
[12] G. Gao, and C. Liang, J. Electrochem. Soc. 154 (2007) 144.
[13] S. S. Mahmoud, J. Mater. Sci. 42 (2007) 989.
[14] M. K. Awad, M. S. Metwally, S. A. Soliman, A. A. El-Zomrawy, and M. A. Bedair, J. Ind. Eng. Chem. 20 (2014) 796.
[15] H. A. El-Dahan, T. Y. Soror, and R. M. El-Sherif, Mater. Chem. Phys. 89 (2005) 260.
[16] I. B. Obot, N. O. Obi-Egbedi, and S. A. Umoren, Corros. Sci. 51 (2009) 276.
[17] A. Y. El-Etre, Corros. Sci. 43 (2001) 1031.
[18] A. S. Fouda, M. N. Moussa, F. I. Taha, and A. I. Elneanaa, Corros. Sci. 26 (1986) 719.

[19] S. M. Hassan, Y. A. Elawady, A. I. Ahmed, and A. O. Baghlaf, Corros. Sci. 19 (1979) 951.
[20] G. Bereket, and A. Yurt, Corros. Sci. 43 (2001) 1179.
[21] G. Gece, Corros. Sci. 53 (2011) 3873.
[22] A. Yurt, S. Ulutas, and H. Dal, Appl. Surf. Sci. 253 (2006) 919.
[23] A. Yurt, and Ö. Aykın, Corros. Sci. 53 (2011) 3725.
[24] Q. B. Zhang, and Y. X. Hua, Mater. Chem. Phys. 119 (2010) 57.
[25] S. S. A. E. Rehim, H. H. Hassaan, and M. A. Amin, Mate.r Chem. Phys. 78 (2002) 337.
[26] A. K. Maayta, and N. A. F. Al-Rawashdeh, Corros. Sci. 46 (2004) 1129.
[27] X. H. Li, S. D. Deng, and H. Fu, Corros. Sci. 53 (2011) 1529.
[28] E. E. F. El-Sherbini, S. M. Abd-El-Wahab, and M. A. Deyab, Mater. Chem. Phys. 82 (2003) 631.
[29] Y. Xiao-Ci, Z. Hong, L. Ming-Dao, R. Hong-Xuan, and Y. Lu-An, Corros. Sci. 42 (2000) 645.
[30] G. Bereket, and A. Pinarbsi, Corros. Eng. Sci. Technol. 39 (2004) 308.
[31] A. S. Fouda, K. Shalabi, and N. H. Mohamed, Int. J. Innov. Res. Sci. Eng. Technol. 3 (2014) 9861.
[32] X. Li, S. Deng, and X. Xie, Corros. Sci. 81 (2014) 162.
[33] P. B. Raja, and M. G. Sethuraman, Mater. Let. 61 (2008) 113.
[34] E. E. Oguzie, Corros. Sci. 49 (2007) 1527.
[35] M. Akram, Shahab-Uddin, A. Aahmed, K. Usmanghani, A. Hannan, E. Mohiuddin, and M. Asif, Rom. J. Biol. Plant Biol. 55 (2010) 65.
[36] J. Jurenka, Altern Med. Rev. 14 (2009) 141.
[37] N. I. Kairi, and J. Kassim, Int. J. Electrochem. Sci. 8 (2013) 7138.
[38] S. Rajendran, K. Duraiselvi, P. Prabhakar, M. Pandiarajan, M. Tamilmalar, and R. J. Rathish, Eur. Chem. Bull. 2 (2013) 850.
[39] K. R. Ansari, M. A. Quraishi, and A. Singh, Corros. Sci. 79 (2014) 5.
[40] C. Verma, P. Singh, I. Bahadur, E. E. Ebenso, and M. A. Quraishi, J. Mol. Liq. 209 (2015) 767.
[41] X. Li, S. Deng, and X. Xie, J. Taiwan Inst. Chem. Eng. 45 (2014) 1865.
[42] M. N. El-Haddad, and A. S. Fouda, J. Mol. Liq. 209 (2015) 480.
[43] K. Krishnaveni, and J. Ravichandran, Trans. Nonferrous Met. Soc. China 24 (2014) 2704.
[44] K. Ramya, R. Mohan, K. K. Anupama, and A. Joseph, Mater. Chem. Phys. 149-150 (2015) 632.
[45] C. Verma, M. A. Quraishi, and A. Singh, J. Taiwan Inst. Chem. Eng. 49 (2015) 229.
[46] K. R. Ansari, and M. A. Quraishi, J. Taiwan Inst. Chem. Eng. 000 (2015) 1.
[47] I. Y. Kuznetsov, Russ. Chem. Rev. 73 (2004) 75.

[48] A. Singh, Y. Lin, W. Liu, D. Kuwanhai, E. E. Ebenso, and J. Pan, Int. J. Electrochem. Sci. 8 (2013) 12851.
[49] N. O. Eddy, H. Momoh-Yahaya, and E. E. Oguzie, J. Adv. Res. 6 (2015) 203.
[50] I. B. Obot, and N. O. Obi-Egbedi, Colloid Surface A 330 (2008) 207.
[51] G. Avci, Mater. Chem. Phys. 112 (2008) 234.
[52] W. H. Li, Q. He, S. T. Zhang, C. L. Pei, and B. R. Hou, J. Appl. Electrochem. 38 (2008) 289.
[53] I. B. Obot, S. A. Umoren, Z. M. Gasem, R. Suleiman, and B. E. Ali. J. Ind. Eng. Chem. 21 (2015) 1328.
[54] N. K. Gupta, C. Verma, M. A. Quraishi, and A. K. Mukherjee, J. Mol. Liq. 215 (2016) 47.
[55] M. A. Amin, Q. Mohsen, and O. A. Hazzai, Mater. Chem. Phys. 114 (2009) 908.
[56] G. K. Gomma, and M. H. Wahdan, Mater. Chem. Phys. 39 (1995) 209.
[57] A. Yurt, S. Ulutas, and H. Dal, Appl. Surf. Sci. 253 (2006) 919.
[58] K. F. Khaled, and M. M. Al-Qahtani, Mater. Chem. Phys. 113 (2009) 150.
[59] L. Garrigues, N. Pebere, and F. Dabosi, Corros. Sci. 41 (1996) 1209.
[60] E. A. Noor, Mater. Chem. Phys. 144 (2009) 533.
[61] G. M. Pinto, J. Nayak, and A. N. Shetty, Mater. Chem. Phys. 125 (2011) 628.
[62] S. D. Deng, and X. H. Li, Corros. Sci. 64 (2012) 253.
[63] J. Bessone, C. Mayer, K. Jutter, and W. Lorenz, Electrochim. Acta 28 (1983) 171.
[64] C. M. A. Brett, Corros. Sci. 33 (1992) 203.
[65] G. T. Burstein, and R. J. Cinderey, Corros. Sci. 32 (1992) 1195.
[66] S. S. A. E. Rehim, H. H. Hassan, and M. A. Amin, Mater. Chem. Phys. 70 (2001) 64.
[67] M. Lebrini, M. Lagrenée, H. Vezin, M. Traisnel, and F. Bentiss, Corros. Sci. 49 (2007) 2254.
[68] M. Lagrenée, B. Mernari, M. Bouanis, M. Traisnel, and F. Bentiss, Corros. Sci. 44 (2002) 573.
[69] W. J. Lorenz, and F. Mansfeld, Corros. Sci. 21 (1981) 647.
[70] L. H. Madkour, and S. K. Elroby, Int. J. Ind. Chem. 6 (2015) 165.
[71] C. Verma, L. O. Olasunkanmi, I. B. Obot, E. E. Ebenso, and M. A. Quraishi, RSC Adv. 6 (2016) 15639.
[72] M. Yadav, S. Kumar, D. Behera, I. Bahadur, and D. Ramjugernath, Int. J. Electrochem. Sci. 9 (2014) 5235.
[73] C. Verma, M. A. Quraishi, L. O. Olasunkanmi, and E. E. Ebenso, RSC Adv. 5 (2015) 85417.
[74] B. Xu, Y. Ji, X. Zhang, X. Jin, W. Yang, and Y. Chen, RSC Adv. 5 (2015) 56049.
[75] C. Verma, M. A. Quraishi, and A. Singh, J. Mol. Liq. 212 (2015) 804.

[76] Y. M. Tang, W. Z. Yang, X. S. Yin, Y. Liu, R. Wan, and J. T. Wang, Mater. Chem. Phys. 116 (2009) 479.
[77] C. Verma, and M. A. Quraishi, J. Assoc. Arab. Univ. Basic. Appl. Sci. 22 (2017) 55.
[78] C. Verma, E. E. Ebenso, I. Bahadur, I. B. Obot, and M. A. Quraishi, J. Mol. Liq. 212 (2015) 209.
[79] G. Y. Elewady, and H. A. Mostafa, Desalination 247 (2009) 573.
[80] S. A. Umoren, and E. E. Ebenso, Mater. Chem. Phys. 106 (2007) 387.